Atmospheres

Supporting Information for

Daytime Oxidized Reactive Nitrogen Partitioning in Western U.S. Wildfire Smoke Plumes

Julieta F. Juncosa Calahorrano[1], Jakob Lindaas[1], Katelyn O'Dell[1], Brett B. Palm[3], Qiaoyun Peng[3], Frank Flocke[2], Ilana B. Pollack[1], Lauren A. Garofalo[4], Delphine K. Farmer[4], Jeffrey R. Pierce[1], Jeffrey L. Collett, Jr.[1], Andrew Weinheimer[2], Teresa Campos[2], Rebecca S. Hornbrook[2], Samuel R. Hall[2], Kirk Ullmann[2], Matson A. Pothier[4], Eric C. Apel[2], Wade Permar[5], Lu Hu[5], Alan J. Hills[2], Deedee Montzka[2], Geoff Tyndall[2], Joel A. Thornton[4], and Emily V. Fischer[1]

1 Department of Atmospheric Science, Colorado State University, Fort Collins, CO, USA
2 Atmospheric Chemistry Observations & Modeling Laboratory, National Center for Atmospheric Research, Boulder, CO, USA
3 Department of Atmospheric Sciences, University of Washington, Seattle, WA, USA
4 Department of Chemistry, Colorado State University, Fort Collins, CO, USA
5 Department of Chemistry and Biochemistry, University of Montana, Missoula, MT, USA

Contents of this file

Table S1. Instrument details and contact information for measurements described in section 2.2

Molecules(s)	**Instrument**	**PI, Contact, Institution, Reference**	**Detection Limit, Uncertainty**
CO	QC-TILDAS	Teresa Campos, campos@ucar.edu, NCAR, (Lebegue et al., 2016)	100 pptv, 0.6 ppbv
CO	Picarro	Teresa Campos, campos@ucar.edu, NCAR,	30 pptv, NA
NO	2-channel chemiluminescence	Andy Wienheimer, wein@ucar.edu, NCAR, (Ridley and Grahek, 1990)	100 pptv, 6%
NO2	2-channel chemiluminescence	Andy Wienheimer, wein@ucar.edu, NCAR, (Ridley and Grahek, 1990)	140 pptv, 12%
HONO	I-CIMS	Joel A. Thornton, joelt@uw.edu, University of Washington, (Lee et al., 2014)	20.5 pptv, 30%
HNO3	I-CIMS	Joel A. Thornton, joelt@uw.edu, University of Washington, (Lee et al., 2014)	13.5 pptv, 30%
Org N(g)	I-CIMS	Joel A. Thornton, joelt@uw.edu, University of Washington, (Lee et al., 2014)	NA, Factor of 2
PAN	PAN-I-CIMS	Frank Flocke, ffl@ucar.edu, NCAR, (Zheng et al., 2011)	20 pptv, 12%
PPN	PAN-I-CIMS	Frank Flocke, ffl@ucar.edu, NCAR, (Zheng et al., 2011)	20 pptv, 12%
*p*NO3	HR-ToF-AMS	Delphine Farmer, Delphine.farmer@colosttate.edu, Colorado State University, (Bahreini et al., 2016)	< 0.12 ug m-3, 35%
NVOC	PTR-ToF-MS	Lu Hu, Lu.hu@mso.umt.edu, University of Montana, (Sekimoto et al., 2017)	NA, 50%
HCN	TOGA	Eric Apel, apel@ucar.edu, NCAR,	5 pptv, 20%

		(Apel et al., 2013)	
CH3CN	TOGA	Eric Apel, apel@ucar.edu, NCAR, (Appel et al., 2013)	10 pptv, 40%
2-methylfuran	TOGA	Eric Apel, apel@ucar.edu, NCAR, (Apel et al., 2013)	5 pptv, 20%
Acrolein	TOGA	Eric Apel, apel@ucar.edu, NCAR, (Apel et al., 2013)	0.5 pptv, 30%
Acrylonitrile	TOGA	Eric Apel, apel@ucar.edu, NCAR, (Apel et al., 2013)	1 pptv, 50%
2,2,4-trimethylpentane	TOGA	Eric Apel, apel@ucar.edu, NCAR, (Apel et al., 2013)	0.5 pptv, 15%
Tetrachloroethene	TOGA	Eric Apel, apel@ucar.edu, NCAR, (Apel et al., 2013)	0.5 pptv, 15%
Chloroform	TOGA	Eric Apel, apel@ucar.edu, NCAR, (Apel et al., 2013)	2 pptv, 15%
HFC-134	TOGA	Eric Apel, apel@ucar.edu, NCAR, (Apel et al., 2013)	1 pptv, 50%
HCFC-22	TOGA	Eric Apel, apel@ucar.edu, NCAR, (Apel et al., 2013)	1 pptv, 50%
jNO_2	HARP-Actinic Flux	Samuel R. Hall halls@ucar.edu, NCAR, (Shetter and Müller, 1999)	$1x10^{-6}$ s^{-1}, 12%
jHONO	HARP-Actinic Flux	Samuel R. Hall halls@ucar.edu, NCAR, (Shetter and Müller, 1999)	$1x10^{-7}$ s^{-1}, 15%

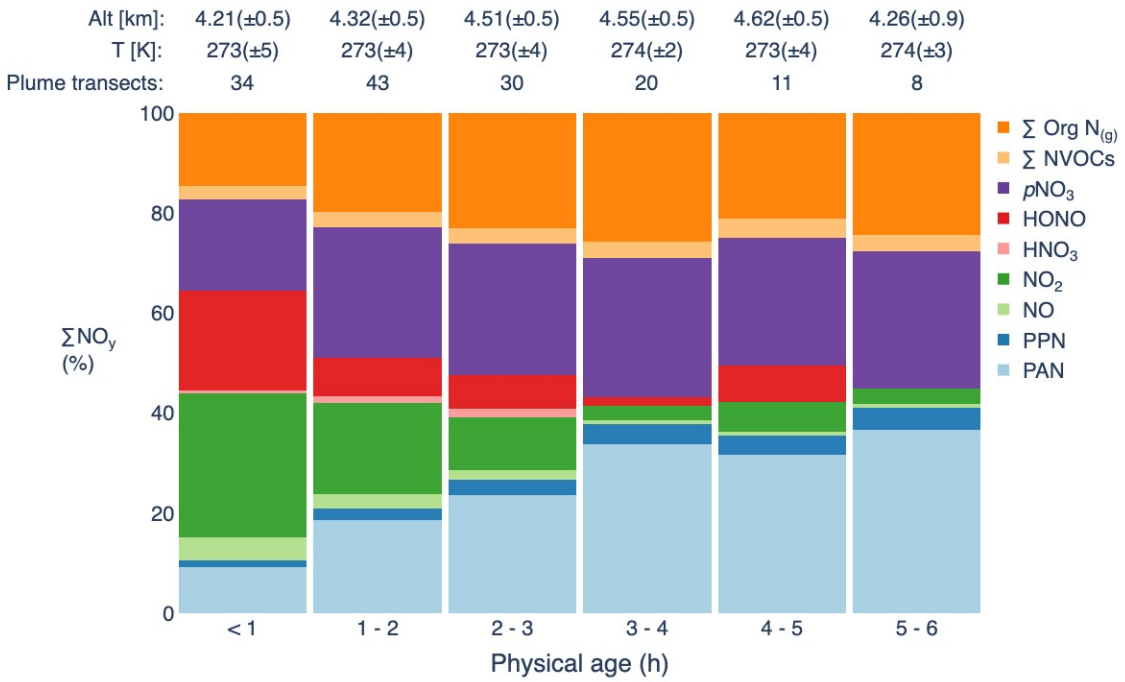

Figure S1. Partitioning of ΣNO_y as a function of physical age (h) in the most concentrated cores of western U.S. wildfire smoke plumes sampled in a pseudo-lagrangian fashion during WE-CAN 2018. Each of the plumes included in this figure are associated with a specifically targeted fire (see Figure 1). The observations shown here correspond to sampling in the center of the plume, which is defined as the portion of each plume transect where CO is above the 75th percentile of that transect. To calculate the enhancement of each species, a crossing-specific background mixing ratio for each individual species is subtracted.

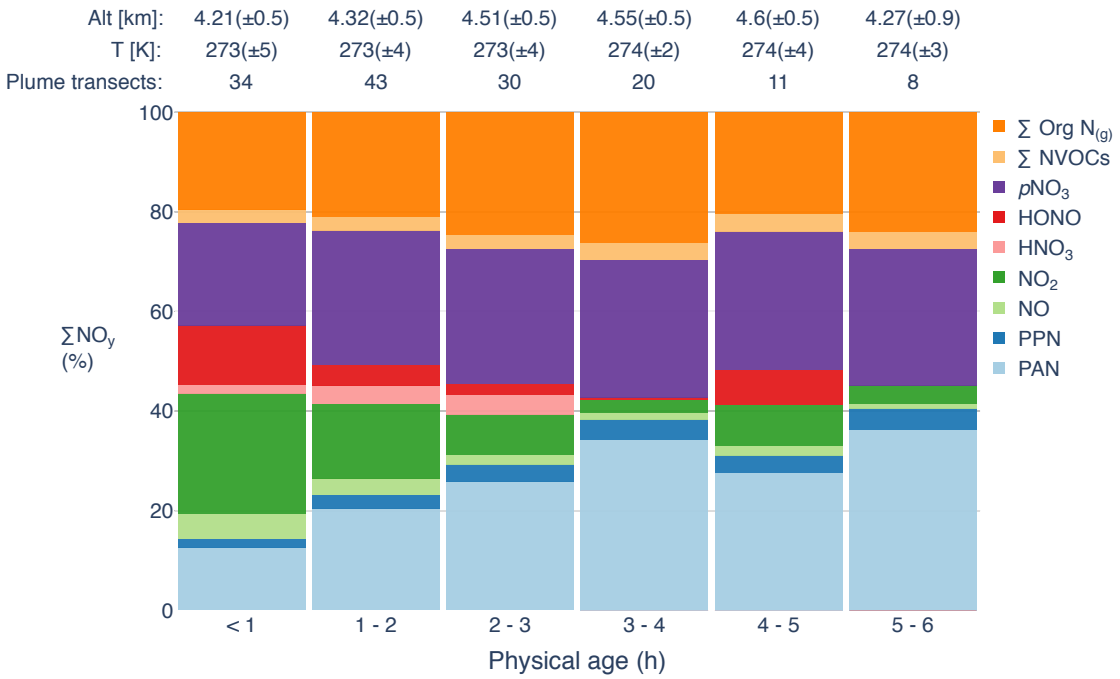

Figure S2. Partitioning of ΣNO_y as a function of physical age (h) outside the most concentrated part of western U.S. wildfire smoke plumes sampled in a pseudo-lagrangian fashion during WE-CAN 2018. Each of the plumes included in this figure are associated with a specifically targeted fire (see Figure 1). The observations shown here correspond to sampling in the portion of each plume crossing where CO is between the 25th and the 75th percentile of that crossing (defined as edges of the plume). To calculate the enhancement of each species, a crossing-specific background mixing ratio for each individual species is subtracted.

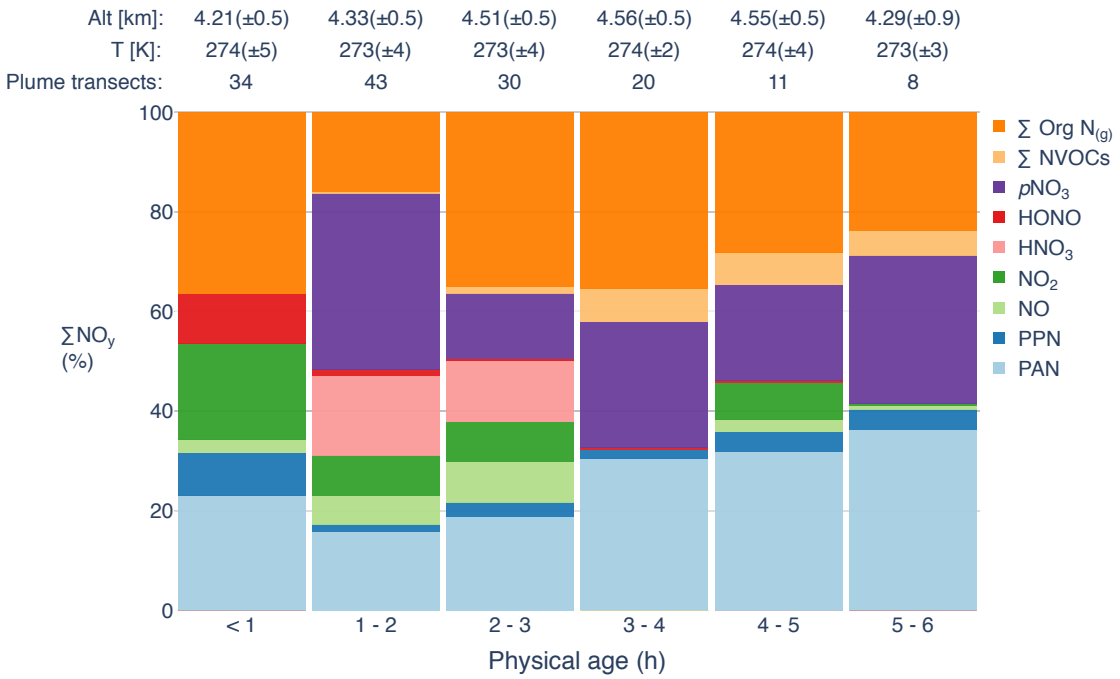

Figure S3. Partitioning of ΣNO_y as a function of physical age (h) in the wings of western U.S. wildfire smoke plumes sampled in a pseudo-lagrangian fashion during WE-CAN 2018. Each of the plumes included in this figure are associated with a specifically targeted fire (see Figure 1). The observations shown here correspond to sampling in the edges of the plume, which is defined as the portion of each plume crossing where CO is between the 5th and the 25th percentile of that crossing (defined as wings of the plume). To calculate the enhancement of each species, a crossing-specific background mixing ratio for each individual species is subtracted.

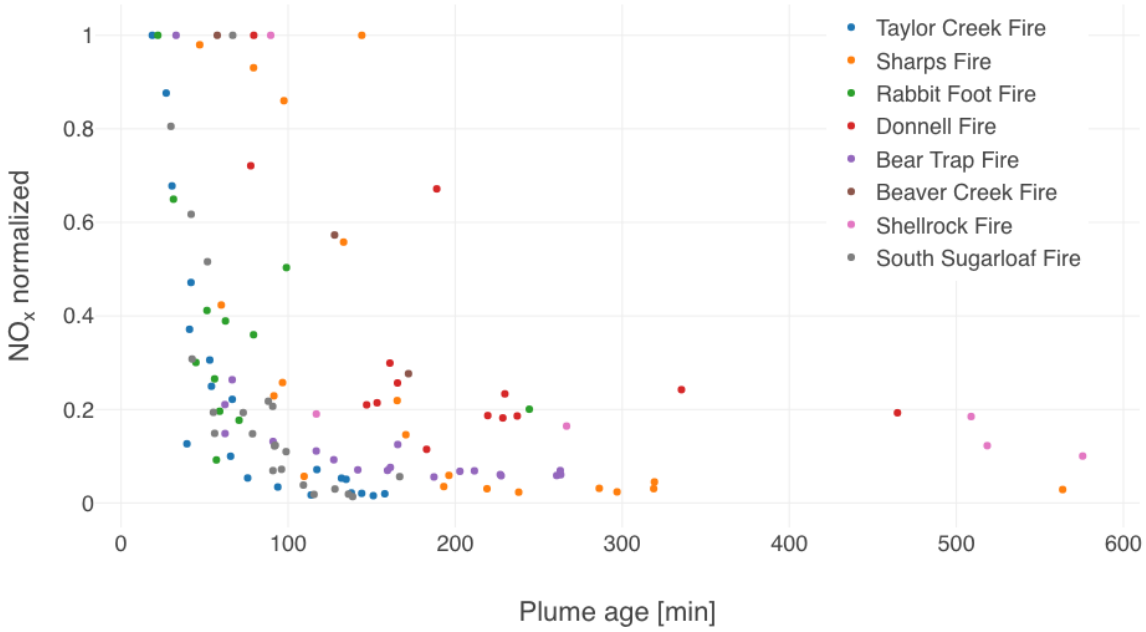

Figure S4. Normalized NO_x in plume cores as a function of plume age [min] for specific fires. The average e-folding time for NO_x is 90 minutes.

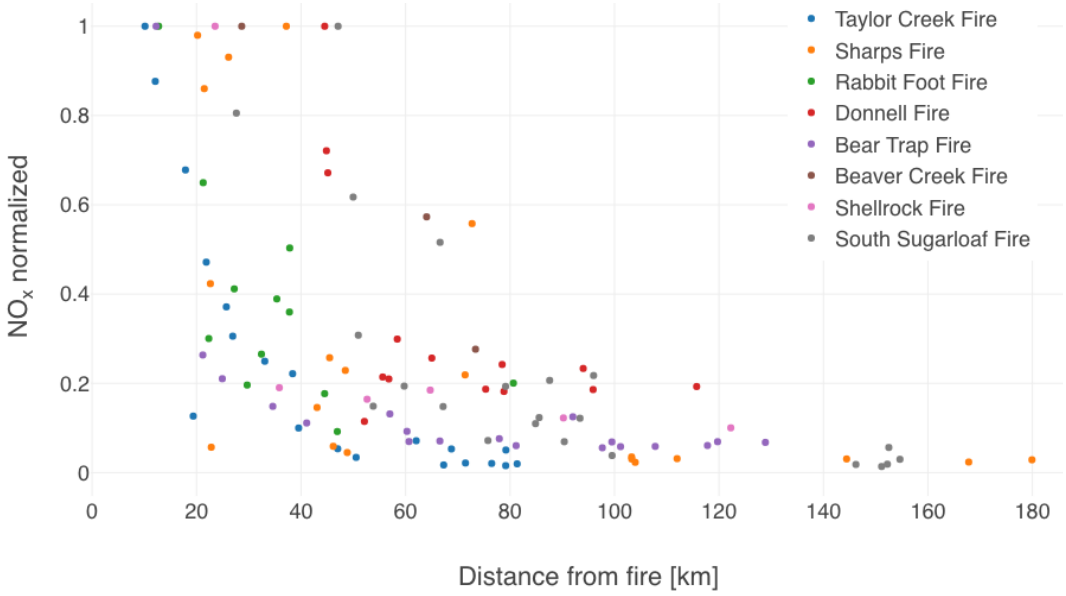

Figure S5. Normalized NO_x in plume cores as a function of distance from the fire [km] for specific fires. The average e-folding distance for NO_x is 40 kilometers downwind.

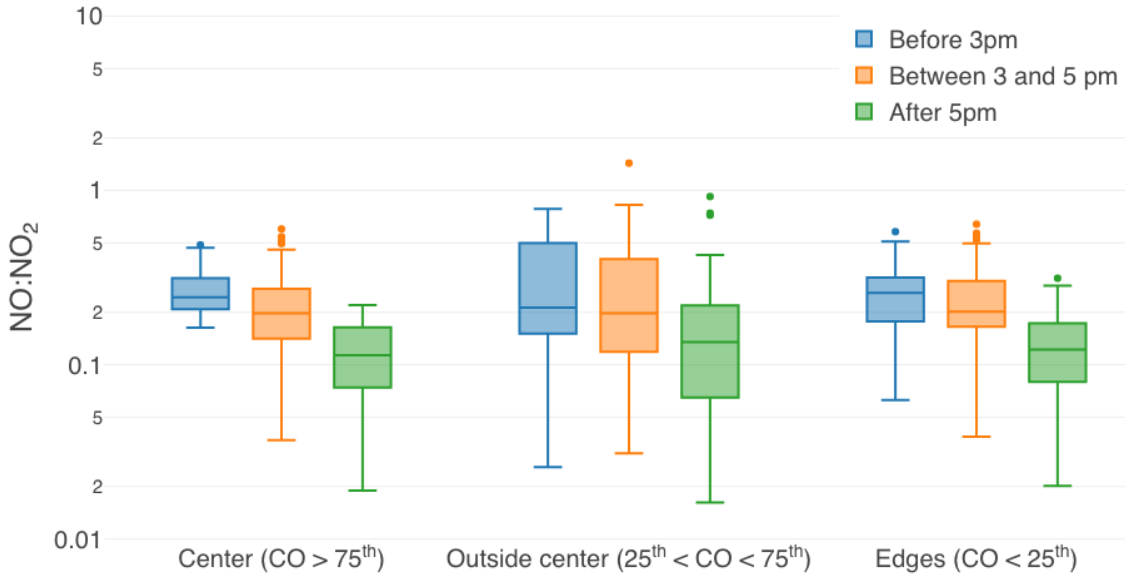

Figure S6. NO to NO_2 ratios in the center, outside the center, and the edges of western US wildfires smoke plumes. The colors of the whisker plots represent different times of the day where blue signifies samples collected before 3 PM (LT), orange signifies samples collected between 3 PM and 5 PM (LT), and green signifies samples collected after 5 PM (LT).

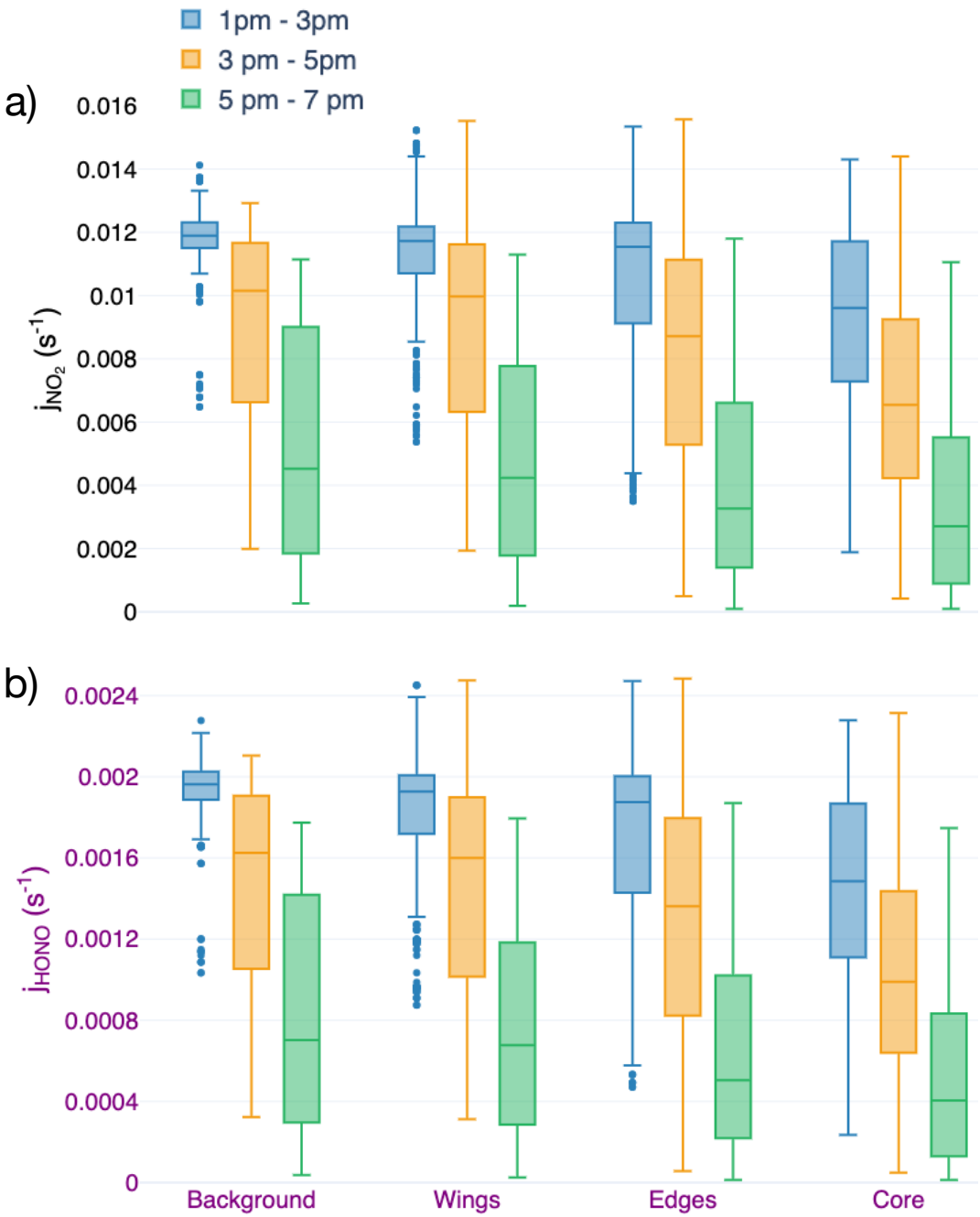

Figure S7. Photolysis rates of a) NO_2 (jNO_2) and b) HONO (jHONO) in the different sections (i.e., cores, wings, edges, and background) of 146 fresh plume transects sampled during WE-CAN (see Section 2.3.1 for details). The core of the plume is defined as the section of a plume transect where CO > 75th percentile. The edges of the plume are defined as the section of a plume transect where 25th > CO > 75th. The wings of the plume are defined as the section of a plume transect where 5th > CO > 25th. Finally, background air is defined as the section of a plume transect where CO < 5th. The colors of the whisker plots represent different times of the day where blue signifies samples collected between 1 and 3 PM (LT), orange signifies samples collected between 3 and 5 PM (LT), and green signifies samples collected between 5 and 7 PM (LT).

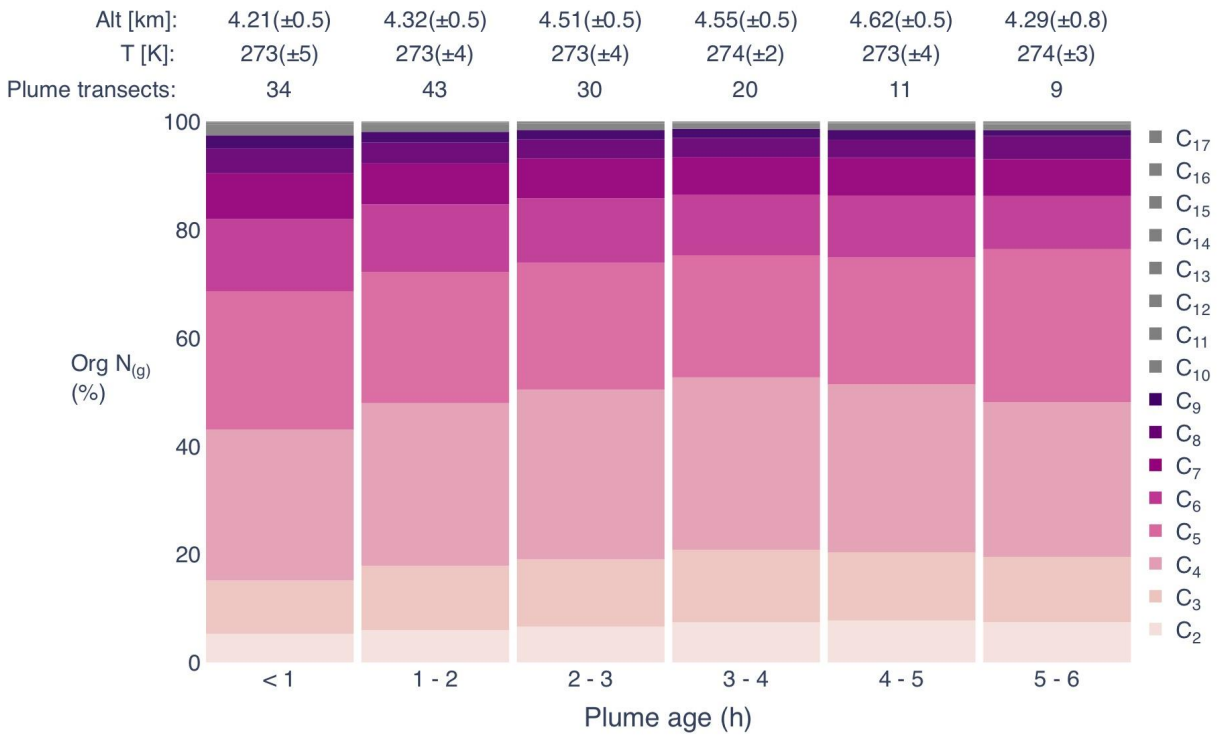

Figure S8. Partitioning of ∑Org N (dark orange bars in Figure 3) as a function of physical age (h) in the western U.S. wildfire smoke plumes sampled in a pseudo-lagrangian fashion during WE-CAN. The different Org N species have been grouped by their carbon atom number. Molecules with > 10 carbon atoms are depicted in grey. Each of the plumes included in this figure are associated with a specifically targeted fire (see Figure 1). The observations shown here correspond to sampling in the entire plume, which is defined as the portion of each plume transect where CO is above the 5th percentile of that transect. To calculate the enhancement of each species, a transect-specific background mixing ratio for each individual species is subtracted.

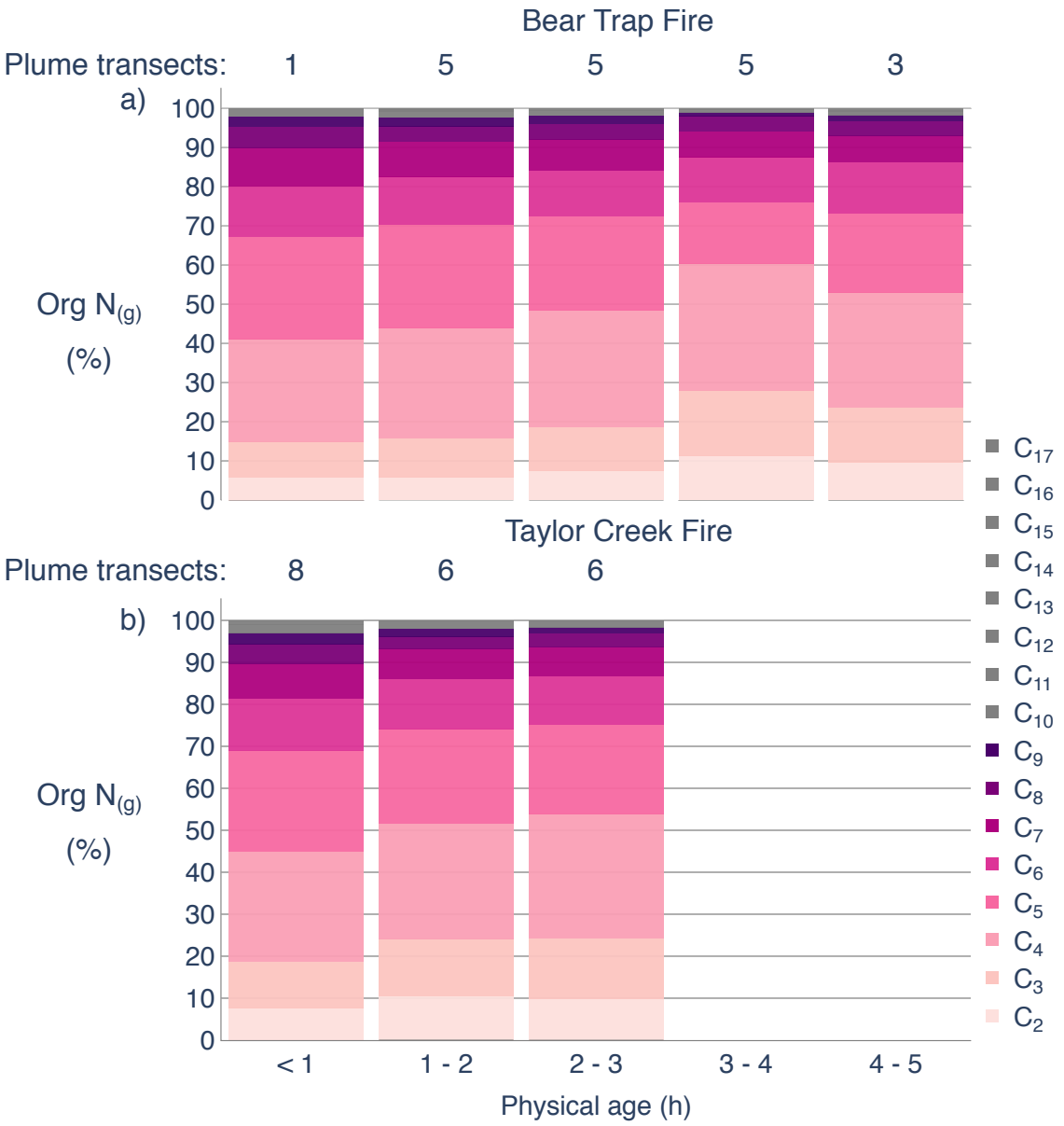

Figure S9. Partitioning of ∑Org N (dark orange bars in Figure 4) as a function of physical age (h) in the Bear Trap Fire and Taylor Creek Fire smoke plumes sampled during WE-CAN. These smoke plumes were sampled in a pseudo-lagrangian fashion twice. Here we present the average of the plume transects from both samples binned by their corresponding physical age. A transect-specific background mixing ratio for each individual species was subtracted. The numbers above each bar signify the individual transects through the plume in each physical age bin.

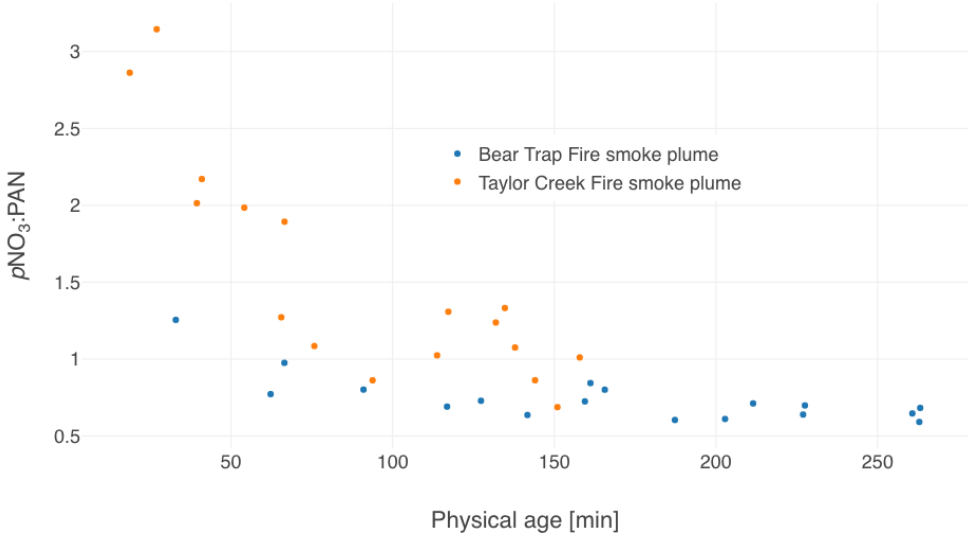

Figure S10. pNO$_3$ to PAN ratios at the core of the plume for the Bear Trap Fire (blue) and the Taylor Creek Fires (orange) smoke plumes as a function of physical age

Text S1

Equation 1 was used to estimate the concentration of OH. X_1 and X_2 are toluene and benzene, respectively. k_1 and k_2 are the rate coefficients for the association reaction with OH for toluene and benzene, respectively.

$$ln\left(\frac{\Delta X1}{\Delta X2}\right)_t = -[OH](k_1 - k_2)t + ln\left(\frac{\Delta X1}{\Delta X2}\right)_0 \quad \text{(Eq. S1)}$$

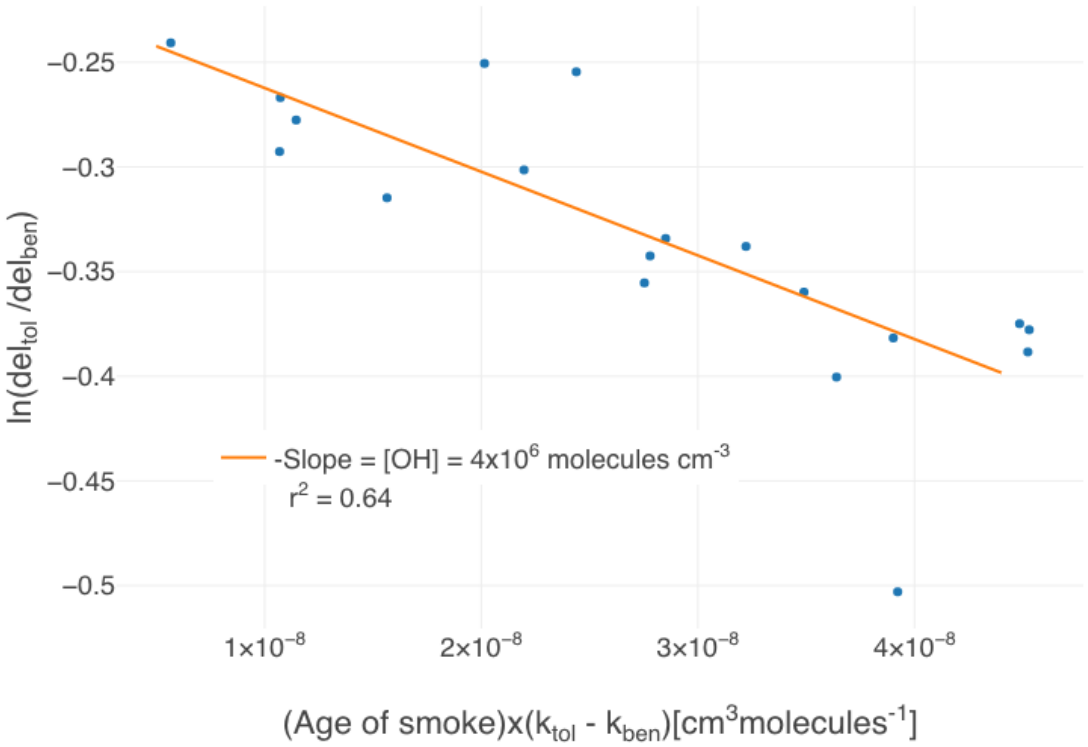

Figure S11. Plot of Eq. S1 for the Bear Trap Fire smoke plume. Mixing ratios for toluene and benzene are at the core of the plume. The slope of the fit provides an estimate for the OH concentration at the core of the plume.

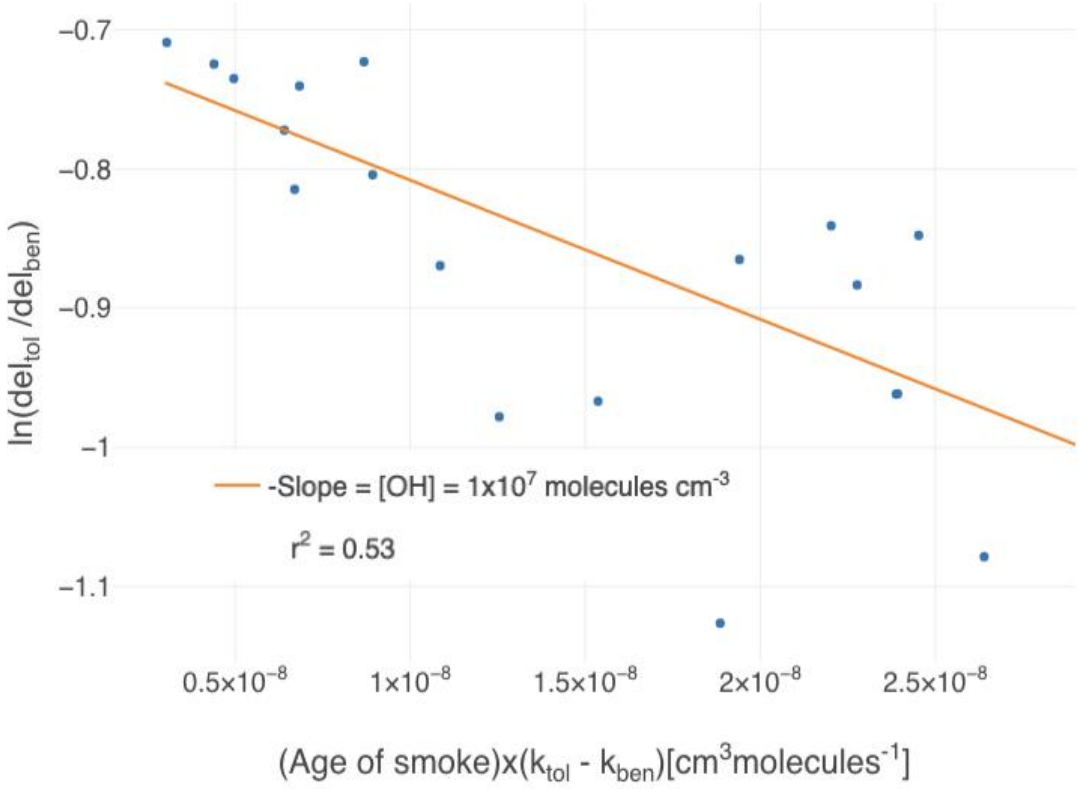

Figure S12. Plot of Eq. S1 for the Taylor Creek Fire smoke plume. Mixing ratios for toluene and benzene are at the core of the plume. The slope of the fit provides an estimate for the OH concentration at the core of the plume.

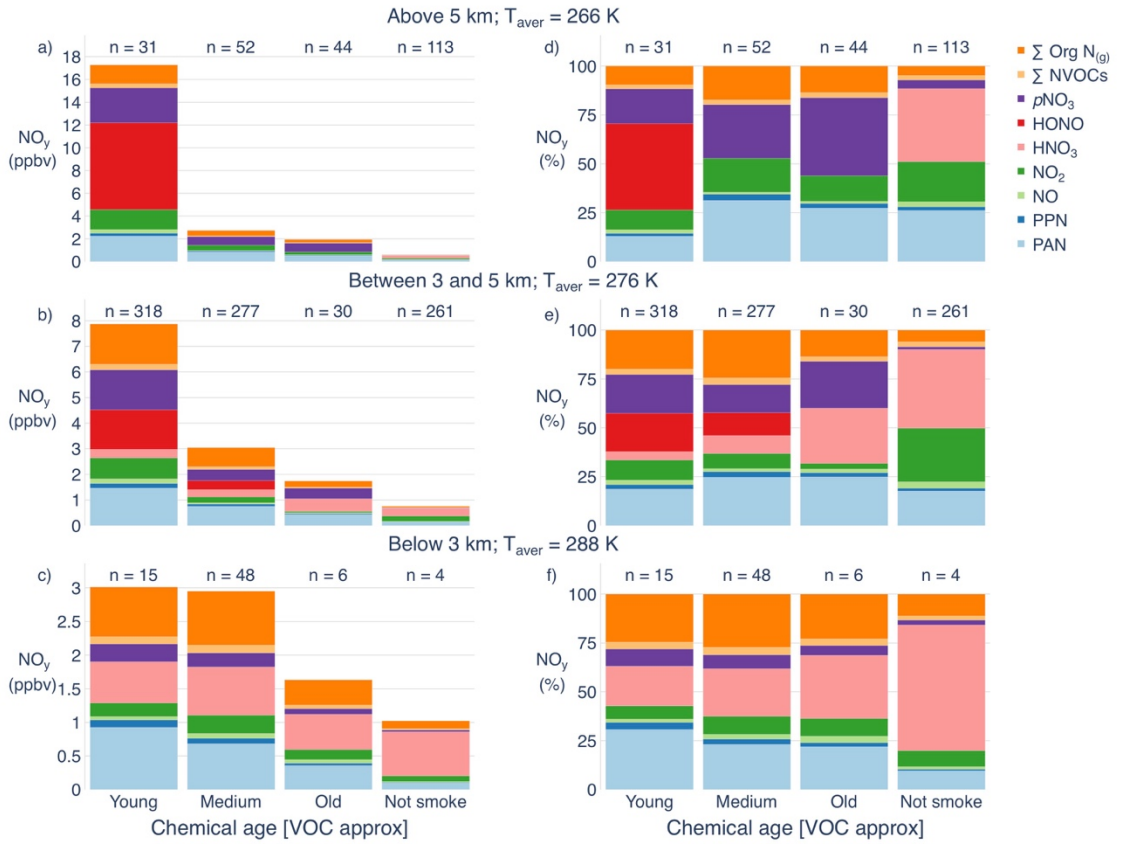

Figure S13. Partitioning of $\sum NO_y$ within smoke-impacted and smoke-free samples within the full WE-CAN dataset. TOGA time-base samples are binned by an approximate chemical age: young (< 1 day of aging), medium (1 - 3 days of aging) and old (> 3 days of aging) as described in Section 2.3.2. Samples are also binned by sampling altitude, and the average temperature of the samples in each category is provided. No background is subtracted; the columns in the left panels represent the partitioning of absolute mixing ratios (note different y-axis) and are shown as percentages in the right panels. The number above each bar represents the number of individual TOGA time segments in category, not individual plume transects. The majority of samples were collected between 3 and 5 km ASL. A smaller number of samples were collected below 3 km, due to safety and logistical constraints of operating the aircraft in low visibility conditions and high terrain elevation on where most of the fires were located. The samples that are substantially influenced by fresh urban emissions (see Section 2.3.2) are not included in this analysis. The scheme described in section 2.3.2 would not identify agriculturally influenced samples. Note that the majority of the young and medium plumes (*i.e.,* left-most bars) coincide with the plumes presented in Figure 3.

Text S2

Briefly, smoke-free samples are characterized by a larger contribution from HNO_3 to $\sum NO_y$ at all altitudes (~40 - 65%, decreases with altitude). Inversely, the pNO_3 contribution to $\sum NO_y$ increases with altitude (consistent with the thermodynamically favorable conditions for NH_4NO_3 formation), but it accounts for a small fraction (<5%) of the $\sum NO_y$ measured. NO_x is between (10-30%) of the $\sum NO_y$ measured with a larger contribution above 3 km (>20%). In the smoke-free WE-CAN samples, PAN and PPN contribution to the $\sum NO_y$ increases with altitude. We note that the WE-CAN smoke-free samples are not broadly representative of the summertime western U.S. atmosphere. The average T/RH/altitude of these samples are 273 K, 20% and 4.5 km ASL respectively and were largely collected outside of urbanized areas.

Across the smoke-impacted dataset, the contribution of HNO_3 to $\sum NO_y$ increases as the plumes age below 5 km. The relative contribution of HNO_3 is largest below 3 km (~20 - 30%). Background mixing ratios have not been subtracted from the data presented in Figure S13, thus the summary of NO_y species include contributions from both smoke and other sources (*e.g.,* anthropogenic emissions and their subsequent chemistry). The relative contribution of smoke is smallest in the most dilute, and often oldest, smoke-impacted air masses. Samples below 3 km also do not carry much weight in the summary of fresh plumes presented in Figure 3. Furthermore, the volatilization of HNO_3 from ammonium nitrate (NH_4NO_3) aerosol into the gas phase is more favorable under warmer temperatures (lower altitudes) (Stelson and Seinfeld, 1982; Matsumoto and Tunaka, 1996). However, there are other potential forms of inorganic and organic pNO_3 in these samples. There is no HNO_3 present in smoke above 5 km, consistent with Figure 3 and the temperature dependency of the NH_3-HNO_3 system that favors NH_4NO_3 at lower temperatures. The measured contribution of pNO_3 to $\sum NO_y$ varies with altitude. Figure S13 shows that, above 3 km, pNO_3 is generally of comparable abundance to NO_x in the younger smoke-impacted samples and more than twice as abundant as NO_x in the old smoke-impacted samples. Below 3 km the pNO_3 contribution decreases as the smoke-impacted samples age and dilute. Between 3 and 5 km (middle row of Figure 5) the

contribution of pNO_3 to $\sum NO_y$ remains approximately constant (~15 - 24%) in all smoke impacted samples, while its contribution increases with more age above 5 km.